Effect of kaolinite modified with Co(II), Cu(II), and Ni(II) salts on selected properties of tread rubber blend

Mariana Pajtášová[1), *)] (ORCID ID: 0000-0001-7834-977X), **Beáta Pecušová[2)]** (0000-0002-7547-5700), **Darina Ondrušová[1)]** (0000-0003-2167-9174), **Ján Vavro[1)]** (0009-0009-6787-9041), **Andrea Feriancová[1)]** (0000-0003-2293-5213), **Silvia Ďurišová[1)]** (0000-0002-2268-7742), **Andrej Dubec[1)]** (0009-0001-6145-6357), **Zuzana Mičicová[1)]** (0000-0002-8803-834X), **Tomasz Waldemar Klepka[3)]** (0000-0001-9182-0845), **Dorota Czarnecka-Komorowska[4)]** (0000-0002-5027-7484)

DOI: https://doi.org/10.14314/polimery.2024.4.6

Abstract: Effect of kaolinite modified with Cu(II), Co(II) and Ni(II) salts as a partial replacement for carbon black (1 and 8 phr) on the properties of the model tread rubber blend was examined. The blends were prepared in a two-stage process in a Brabender mixer at temperatures of 120°C and 100°C, respectively, with a constant mixing speed of 50 rpm. FT-IR confirmed the formation of copper hydroxyacetate monohydrate complex, which may indicate chemical interactions between rubber components and modified kaolinite. The filler improved technological parameters, tensile properties and hardness. Resistance to thermal aging has also increased.

Keywords: kaolinite, rubber blend, FT-IR spectroscopy, curing, mechanical properties.

Wpływ kaolinitu modyfikowanego solami Co(II), Cu(II) i Ni(II) na wybrane właściwości mieszanki gumowej bieżnika

Streszczenie: Zbadano wpływ kaolinitu modyfikowanego solami Cu(II), Co(II) i Ni(II) jako częściowego zamiennika sadzy (1 i 8 phr) na właściwości modelowej mieszanki gumowej bieżnika. Mieszanki przygotowano w dwuetapowym procesie w mieszalniku Brabender w temperaturze odpowiednio 120°C i 100°C, przy stałej prędkości mieszania 50 obr./min. Metodą FT-IR potwierdzono utworzenie kompleksu monohydratu hydroksyoctanu miedzi, co może świadczyć o oddziaływaniach chemicznych pomiędzy składnikami kauczuku i modyfikowanym kaolinitem. Napełniacz poprawił parametry przetwórcze, właściwości mechaniczne przy rozciąganiu i twardość. Zwiększyła się również odporność na starzenie termiczne.

Słowa kluczowe: kaolinit, mieszanka gumowa, spektroskopia FT-IR, wulkanizacja, właściwości mechaniczne.

Polymer nanocomposites are materials consisting of polymer matrix with dispersed nanoparticles or nanofillers, commonly to reduce its cost and improve the mechanical and physical properties. The fillers added to the polymer blend (such as carbon black, silica) positively affect performance properties of the polymer matrix, in comparison with the unfilled polymer. Considerable progress in improving the properties of composites has been proved by the application of nanofillers and the preparation of nanocomposites [1–5]. Recently, common practice is to replace carbon black and silica, which are mostly used in rubber blends, using a small amount of nanofillers, such as layered phyllosilicates in order to achieve a desirable combination of properties. In typical polymer-clay nanocomposites, the filler concentration hardly exceeds 10 phr, whereas in common rubber composites the reinforcing fillers are often used above 30 wt% [6, 7]. Polymer nanocomposites filled with clay minerals, such as kaolinite, are used within various types of industries, e.g., at automotive, textile, space and others. Kaolinite as a material, possess several unique features that set them apart from other adsorbents, such as small grain size, layered structure, high aspect ratio, high specific area, and low levels of impurities. In addition, kaolinite is a widely available low-cost material with high

[1)] Alexander Dubček University of Trenčín, Faculty of Industrial Technologies in Púchov, I. Krasku 491/30, 020 01 Púchov, Slovak Republic.

[2)] Centre for Functional and Surface Functionalized Glass, Alexander Dubček University of Trenčín, Študentská 2, 91150 Trenčín, Slovak Republic.

[3)] Department of Technology and Polymer Processing, Faculty of Mechanical Engineering, Lublin University of Technology, ul. Nadbystrzycka 38d, 20-618 Lublin, Poland.

[4)] Faculty of Mechanical Engineering, Poznan University of Technology, ul. Piotrowo 3, 60-965 Poznan, Poland.

[*)] Author for correspondence: mariana.pajtasova@tnuni.sk

chemical and mechanical stability and good modification [1, 2, 5]. Among them, the improvement of abrasion properties, mechanical performance, stability against heat and improvements in processing of rubber blends are the most important. Kaolinite and its modified forms can be an alternative material for obtaining functional clays-based composites with novel properties in comparison with conventional materials [2, 8–11].

According to the filled area between the individual layers and type of the layer, clay minerals can be divided into three main groups: the group of kaolinite (formatted by feldspar weathering), the group of smectite (e.g. montmorillonite), and the group of iolite (formatted by the decay of feldspar and mica) [10, 12]. Besides the majority of mineral kaolinite, the natural kaolin can contain, other phyllosilicates and feldspars, and other minerals, such as quartz, rutile, hematite, carbonates, sulfides, and various ferrous and aluminum, hydroxides and others that leads into negative impact of its use in industry application, therefore it is recommended to purify the kaolinite mineral by milling and floating [13, 14]. Kaolinite is a layered 1:1 dioctahedral phyllosilicate with the ideal chemical composition of $Al_2Si_2O_5(OH)_4$ [15–17] or it consists of 46.54% of SiO_2, 39.50% of Al_2O_3, and up to 14% of H_2O [18]. The base structure of kaolinite consists of pseudohexagonal crystal units [19]. The distance between a plane of sheet and in the same plane adjacent the sheet is known as the basal spacing that is 0.72 nm in the kaolinite [20–24].

The basic structural layer of kaolinite can be described as one tetrahedral network with central silicon atoms and one octahedral network with central aluminum atoms via the sharing oxygen atoms [10, 19, 25, 26]. The crystal framework of kaolinite is usually devoid of isomorphic substitutions. Due to its low cation exchange capacity, kaolinite is difficult to modify. To improve the properties of kaolinite, methods such as acid/base activation, calcination, intercalation of organic blends, microwave and ultrasonic treatment are used [27–29].

The most reactive functional groups in kaolinite are hydroxyl groups, which are capable of taking part in many chemical reactions as well as modification processes. The intercalation opens access to basal surface for reagents to interact with atoms of basal surface, usually through physical forces, mostly having hydrogen bond origin. Although the kaolinite layers are held together through hydrogen bonds, some high polar organic molecules, for example potassium acetate, dimethyl sulfoxide (DMSO), urea, and formamide can be intercalated into the kaolinite structure [2, 30–32]. These molecules are divided into three types:

– blends, such as urea or formamide which contain two distinct groups to accept and donate hydrogen;

– blends with a high dipole moment, such as dimethyl sulfoxide;

– ammonium, potassium, or cesium salts of short-chain fatty acids [33, 34].

Feriancová *et al.* [35] modified commercial kaolinite with treatment by copper acetate in presence of NaOH. Using this method, a copper complex was formed in the structure of kaolinite. Authors found that this complex could affect the interactions between kaolinite and other rubberizing components. Furthermore, Cu(II) kaolinite filler had positive effect on the mechanical properties of studied natural rubber (NR) blends in amount of 5 and 10 wt%.

Therefore, the work presented in this paper is focused on investigating the effect of Co(II), Cu(II) and Ni(II) acetate salts as a kaolinite filler on the processing, vulcanization, and mechanical properties of kaolinite/styrene butadiene rubber (SBR) blends and its application in rubber industry.

EXPERIMENTAL PART

Materials

The modified kaolinite, named KKA-Co, KKA-Cu, KKA-Ni, were prepared using chemical treatment from commercial kaolin (LB Minerals, Ltd., Kaznějov, Czech Republic), which crystallographic structure is presented in Fig. 1. The chemical composition of kaolinite was as follows: SiO_2 60.01 wt%, Al_2O_3 34.54 wt%, K_2O 1.84 wt%, SO_3 0.86 wt%, TiO_2 1.09 wt%, Fe_2O_3 0.57 wt%, V_2O_5 0.03 wt% at 8.62% LOI. Potassium acetate, copper acetate, cobalt acetate and nickel acetate were purchased from Merck (Rahway, NJ, USA). All chemicals used were of analytical grade. The main polymer matrix was Kralex 1723 synthetic rubber (Synthos SA, Oswiecim, Poland) filled with a commercial N339 carbon black filler (MAKROchem, Lublin, Poland). Zinc oxide (SlovZinc, a.s., Košeca, Slovakia) with a density of 5.5–5.7 g/cm^3, stearic acid (Aldrich Chemical Company Inc., Burlington, MA, USA) with a density of 0, 94 g/cm^3, RAE plasticizer (Shell Slovakia, Bratislava, Slovakia) with a density of 0.96–1.00 g/cm^3, N sulfur (Istrochem a.s., Bratislava, Slovakia), CBS accelerator sulfenax (Istrochem a.s., Bratislava, Slovakia) , DPG as an accelerator (Akrochem Corporation, Akron, OH, USA) and antioxidant (Dusantox, Duslo a.s., Administratívna budova, Šaľa, Slovakia) with a density of 1.06 g/cm^3 were used. Modified kaolinite was used instead of N339. It was added in amounts of 1 phr and 8 phr as follows: Co/1, Co/8; Cu/1, Cu/8; Ni/1, Ni/8, regarding the samples description. Here the original blend stands for ST.

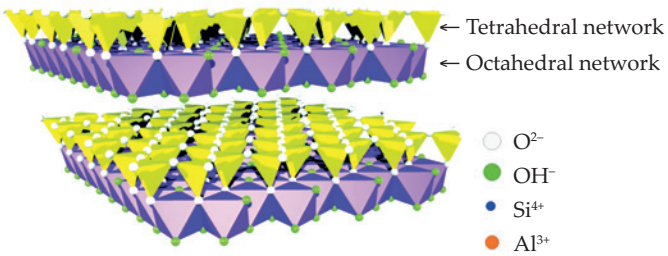

Fig. 1. Structure of kaolinite

a)

b)

c)

Fig. 2. Preparation of modified kaolinite: a) KKA-Co, b) KKA-Cu, c) KKA-Ni

Preparation of modified kaolinite

KKA was chemically treated with 0.5 M potassium acetate solution (CH_3COOK) at 60°C and stirred for 7 hours using a magnetic stirrer at 500 rpm. The obtained dispersion was washed many times to remove the excess salts, than dried at 60°C and sieved through a sieve with a mesh diameter of 25 μm. Then, kaolinite modified with Co(II), Cu(II) and Ni(II) salts was prepared from the sieved dispersion and 0.5 M solutions of $Co(CH_3COO)_2{\cdot}4H_2O$, $Cu(CH_3COO)_2{\cdot}H_2O$ and $Ni(CH_3COO)_2{\cdot}4H_2O$. The pH was controlled with 0.3 M NaOH solution. Vigorous stirring was performed for 24 hours. The excess acetate solution was removed by washing with distilled water. Then, the samples were filtered and dried in air and in an oven. Finally, the prepared product was crushed and, after

T a b l e 1. Chemical composition of pure and modified kaolinite

Sample	Composition, wt%								
	SiO_2	Al_2O_3	K_2O	TiO_2	SO_3	P_2O_5	CoO	CuO	NiO
KKA	60.29	35.10	1.50	1.06	0.81	0.60	–	–	–
KKA-Co	60.07	32.73	1.54	1.11	0.86	0.70	2.37	–	–
KKA-Cu	58.85	34.31	1.46	1.00	0.77	0.56	-	2.48	-
KKA-Ni	61.13	32.01	1.55	1.10	0.74	0.60	–	–	2.23

T a b l e 2. Selected IR bands of the fillers

Type of vibration	Wavenumber, cm^{-1}				References
	KKA	KKA-Cu	KKA-Co	KKA-Ni	
$\nu_{1\text{-}3}$(OH)	3687, 3669, 3650	3687, 3668, 3650	3687, 3668, 3650	3687, 3668, 3649	[36]
ν_5(OH)	3618	3618	3618	3618	[36]
$\nu_{as}(COO^-)$	–	1559	1560	1560	[36, 40]
$\nu_{sym}(COO^-)$	–	1408	1420	1420	[36, 40]
ν(Si-O)ap	1113	1113	1113	1113	[35, 36]
ν(Si-O)	1025, 1001	1025, 1000	1025, 1000	1025, 1000	[37]
δ(Al-Al-OH)	910	910	910	910	[35, 41]
δ(Si-O-Al)	529	528	528	526	[42]
δ(Si-O-Si)	460	456	456	456	[42]

drying, sieved (Fig. 2). A 25 μm sieving undersize was used for all following experiments.

Methods

Chemical structure

Infrared spectra were recorded, using FT-IR Nicolet iS50 Thermo Scientific (Waltham, MA, USA) spectrometer in the 4000–400 cm^{-1} range, with a spectral resolution of 4 cm^{-1}. The measurements were made by ATR technique, using diamond crystal. X-ray powder diffraction (XRD) patterns were recorded with Panalytical Empyrean (Malvern, United Kingdom) with special software under following conditions: CuKα wavelength, power consumption of 45 kW, in the region between 5 and 70° 2θ, in a step of 0.05° and a measurement time of 1 s in one position. The EDX analysis was carried out with the energy-dispersive fluorescence X-ray spectrometer (Shimadzu EDX-7000, Kyoto, Japan). Scanning electron microscopy (SEM) images were taken using Tescan VEGA 3 (Brno, Czech Republic) microscope with BSE detector and field of view 40 mm with Wide Field Optics (7000–20 000 magnification).

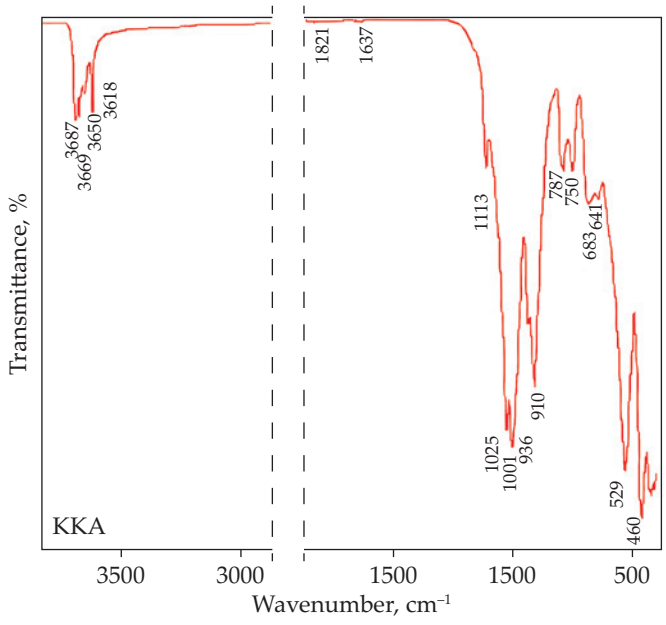

Fig. 3. Infrared spectrum of KKA in selected regions

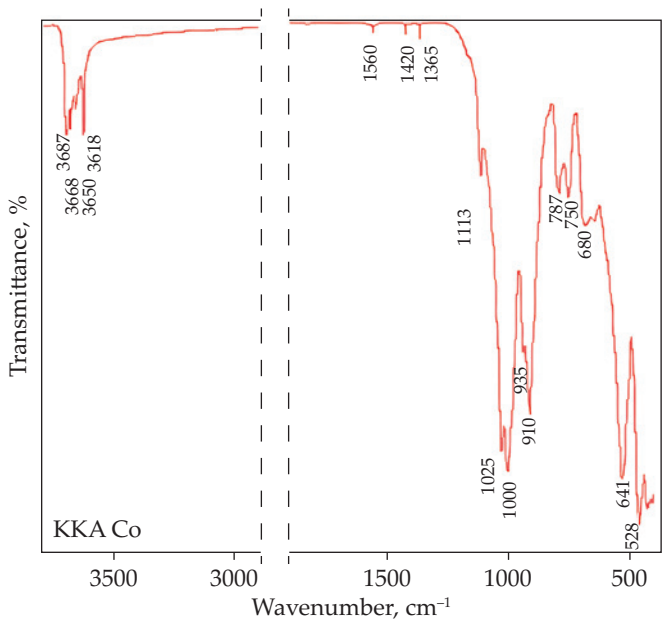

Fig. 4. Infrared spectrum of KKA-Co in selected regions

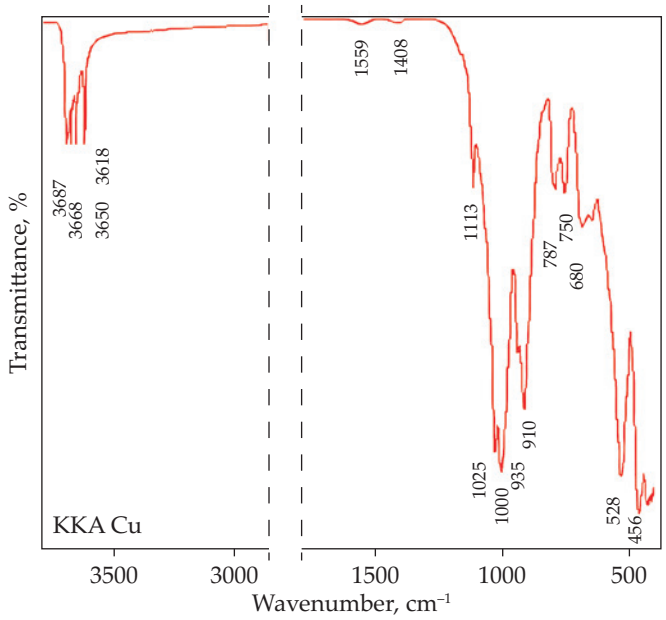

Fig. 5. Infrared spectrum of KKA-Cu in selected regions

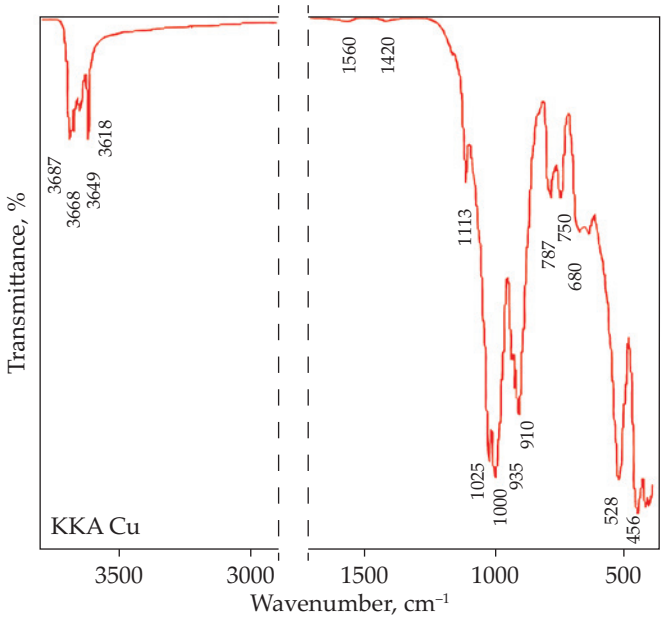

Fig. 6. Infrared spectrum of KKA-Ni in selected regions

The model rubber tread blends were prepared during two step mixing process in Plasti-corder Brabender EC Plus (Duisburg, Germany). A temperature of 120°C was used in the first step of mixing and 100°C was in the second step of mixing with a constant speed of 50 rpm. The processing characteristics and curing properties were measured by Rubber Process Analyzer (RPA 2000 Alpha Technologies, Akron, OH, USA) at a test temperature of 160°C for 30 min following ISO 6202-3 standard.

Curing characteristic

Determination of cure characteristics is based on measuring the maximum and minimum torque under shear deformation over time at a specific temperature. The test chamber mold was opened after reaching a specific temperature and then, the test sample in a shape of a circle was put inside. The chamber was closed, and rotor was launched. The moment of closing the test chamber was registered as the cure beginning with recording of curing's curve. The difference between maximum torque M_H and minimum torque M_L is called delta torque ΔM. Curing rate coefficient (CRI) is the parameter corresponding to the inductive period length according to the Equation 1.

$$CRI = \frac{100}{t_{90} - t_{s2}} \tag{1}$$

where: t_{90} is optimal cure time and t_{s2} safety processing (scorch time) parameter.

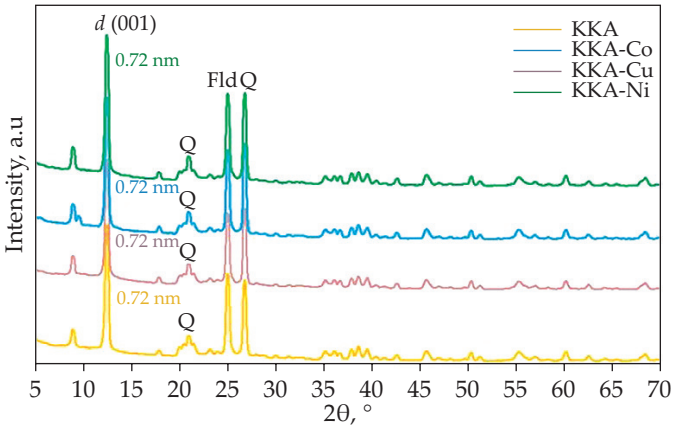

Fig. 7. XRD diffraction patterns of pure and modified kaolinite

Mechanical properties

Tensile properties were determined according to ISO 37 using a testing machine Shimadzu Autograph AG-X plus (Kyoto, Japan) at constant speed of 500 mm/min. Paddle-shaped samples were used. Hardness was tested using digital Shore A hardness tester according to ISO 48-4. A cylindrical sample with a diameter of 50 mm and a thickness of 6 mm was used for testing.

Thermal aging

The test of accelerated thermal aging was performed for 72 hours at the temperature of 100°C. The change of physical properties S was determined according to the Equation 2, where A_0 is the value of physical properties before accelerated thermal aging in air and A_1 is the value of physical properties after accelerated thermal aging in air.

$$S = \frac{A_1 - A_0}{A_0} \cdot 100\% \tag{2}$$

The change of hardness value ΔH (%) was determined by following Equation 3, where H_0 is the value of hardness before accelerated thermal aging and H_1 is the value of hardness after accelerated thermal aging.

$$\Delta H = H_1 - H_0 \tag{3}$$

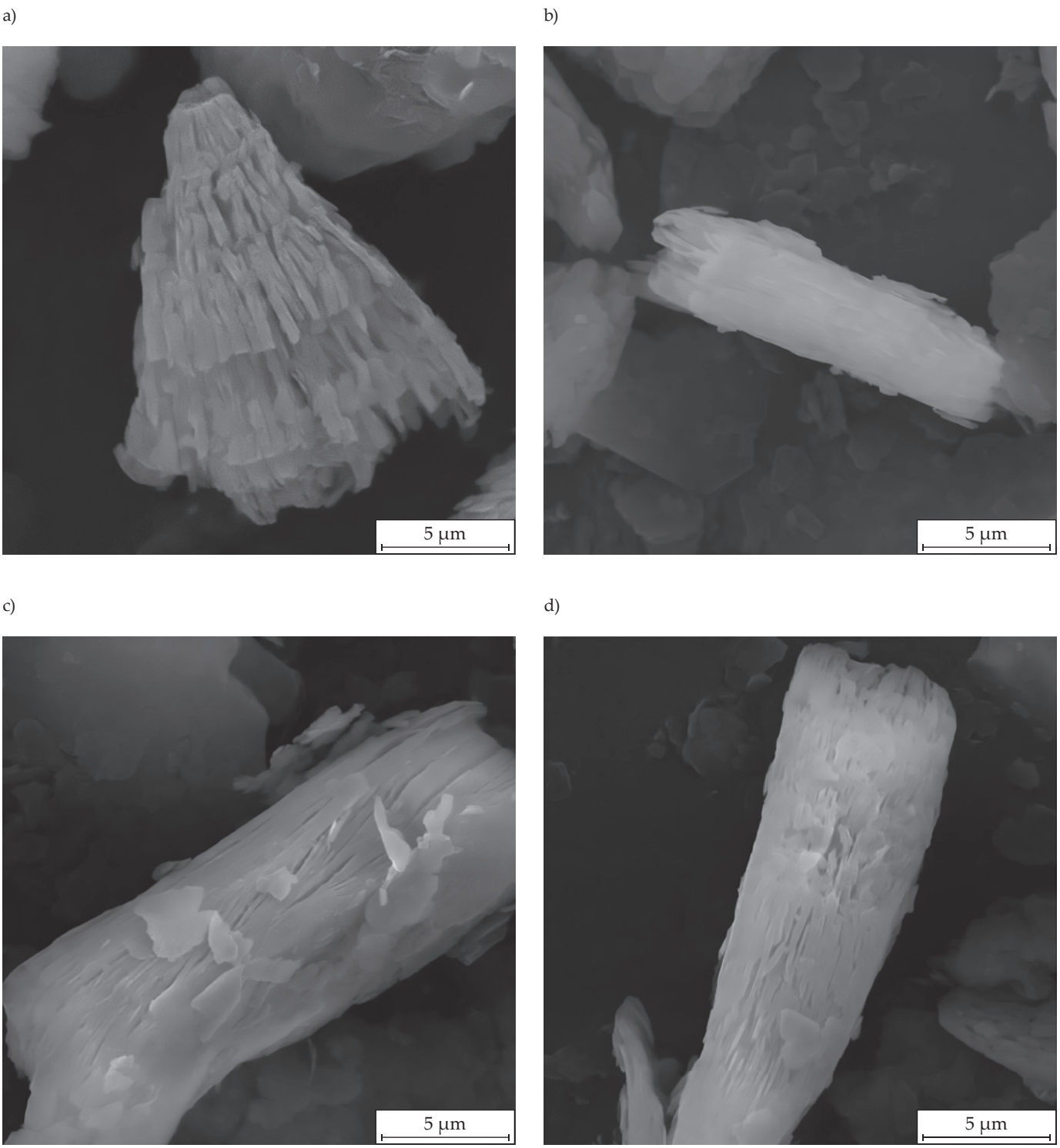

Fig. 8. SEM micrographs of kaolinite: a) KKA, b) KKA-Co, c) KKA-Cu, d) KKA-Ni

RESULTS AND DISCUSSION

Fillers characteristic

EDX was used to characterize the chemical composition of kaolinite and the subsequent chemical changes that occurred due to modification of kaolinite (Tab. 1). Kaolinite contains mostly SiO_2, Al_2O_3, while other oxides such as K_2O, TiO_2, SO_3 are present in lower amounts. After the treatment of kaolinite by Co(II), Cu(II), Ni(II) acetates, a slight decrease in silica and alumina content was observed and Co, Cu, and Ni content at the same time and it can be expressed as CoO, CuO, and NiO.

The infrared spectra of modified kaolinite are shown in Figs. 3–6 and selected vibrations are listed in Table 2. In the FT-IR spectrum of KKA the outer and inner stretching vibrations of surface hydroxyl groups $\nu(OH^-)$ at 3687 cm^{-1}, 3669 cm^{-1} and 3650 cm^{-1} and inner $\nu(OH^-)$ stretching vibration at 3618 cm^{-1} can be seen. Then, outer stretching vibrations $\nu(OH^-)$ of kaolinite modified forms

T a b l e 3. Processing parameters and curing characteristic of the rubber blends

Sample	M_L Nm	M_H Nm	ΔM Nm	t_{s2} min	t_{90} min	CRI min^{-1}
ST	1.7	12.3	10.6	1.7	5.8	24.7
Co/1	1.9	12.0	10.1	1.8	6.5	21.4
Co/8	1.6	11.8	10.1	2.1	5.6	28.5
Cu/1	2.0	11.5	9.8	1.7	5.8	24.8
Cu/8	1.6	11.1	9.5	2.2	7.2	20.1
Ni/1	1.8	10.9	9.1	2.0	5.9	25.7
Ni/8	1.4	10.6	9.1	1.8	4.8	32.5

occurred at 3687 cm^{-1}, 3668 cm^{-1}, 3650 cm^{-1}, 3649 cm^{-1} and inner $\nu(OH^-)$ occurred also at 3618 cm^{-1} [36-38]. Bending vibrations of hydroxyl groups (δOH^-) of kaolinite and its modified forms were seen at 910 cm^{-1} [36]. The ATR spectra of KKA-Cu, KKA-Co, KKA-Ni samples show the presence of new absorption bands at 1560 cm^{-1} and 1408–1420 cm^{-1} which are related to the asymmetric and symmetric stretching vibrations of $\nu_{as}(COO^-)$ and $\nu_s(COO^-)$ carboxylate group [41, 42]. Herein, the difference between the $\nu_s(COO^-)$ and $\nu_{as}(COO^-)$ is 151 cm^{-1} (for KKA-Cu) and 140 cm^{-1} (for KKA-Co, KKA-Ni) relates to the formation of the complex in the modified forms of kaolinite [35, 42]. The stretching vibration of ν(Si-O) can be seen at 1025 cm^{-1}. Deformation vibrations δ(Si-O-Al) and δ(Si-O-Si) can be seen between 528 cm^{-1} to 526 cm^{-1} and 456 cm^{-1}, respectively [42].

All diffraction patterns of pure and modified KKA showed a strong diffraction peak at $2\theta = 12.35°$, as seen in Fig. 7. The d001 reflection indicates the main mineral kaolinite and corresponds to a basal space of $d = 0.72$ nm for all samples. Quartz (Q) and feldspar (Fld) diffraction maximum were identified within the analysis. Nonetheless, in the diffraction pattern of KKA-Cu, new diffraction peaks at $2\theta = 5.6°$ with the value of $d = 1.592$ nm is observed. According to literature data, this value confirmed the assumption that a new complex with a lamellar structure was created as a result of kaolinite modification. No significant changes were observed in the basic structure spacing in the layered kaolinite structure [35, 41, 43].

SEM analysis allows to estimate the average thickness of individual layers and the size of the gap, which are 0.27 μm and 0.34 μm, respectively. Analysis also confirmed the presence of a layered structure of the kaolinite powder form. As it can be seen in Fig. 8a, it is possible to observe a larger gap between the individual layers. The surface microrelief is characterized by a strong micromorphology and it is possible to observe a number of free fragments on the surface. The individual layers are arranged irregularly with considerable differences in their thickness. The orientation of layers is not strictly linear, their curved shape as well as the presence of a large number of well-defined segments are manifested in several places as it can be seen in Fig. 8a.

Average thickness of individual layers of KKA-Co microstructure, based on 2D measurements are approximately 0.16 μm without visible gaps. The analyzed sample of modified kaolinite KKA-Co form (Fig. 8b) consists of a layered structure with a tight arrangement of individual layers. The microstructure interstitially was not observed. The surface micromorphology is not similar as in the KKA sample (Fig. 8a). There are almost no layer fragments present in relation to the observed particle surface. The individual layers are arranged more regularly, more or less linearly, with little occurrence of their curvature and no significant differences in their thickness. A significant segmentation of the layers is not visible for the surface of the particle. Geometric parameters of KKA-Cu microstructure, based on 2D measurements, performed for specific images, are average thickness of individual layers – approximately 0.15 μm and gap size – approximately 0.20 μm. The layered structure of the KKA-Cu sample is characterized by a visible gap between the individual layers, as it can be seen in Fig. 8c. Microrelief with a visible micromorphology is observed for the particle completed by the presence of a large number of segments on the layer's surface. The individual layers are arranged more nonlinearly, their curved shape is observed in several areas. The thickness of the layers is smaller and without significant differences between the individual layers. Geometric parameters of KKA-Ni microstructure, based on 2D measurements, performed for specific images, are average thickness of individual layers – approximately 0.14 μm and the gap is not observed. The KKA-Ni sample, shown in Fig. 8d, is characterized by a tight arrangement of the layered structure without visible gap between the individual layers.

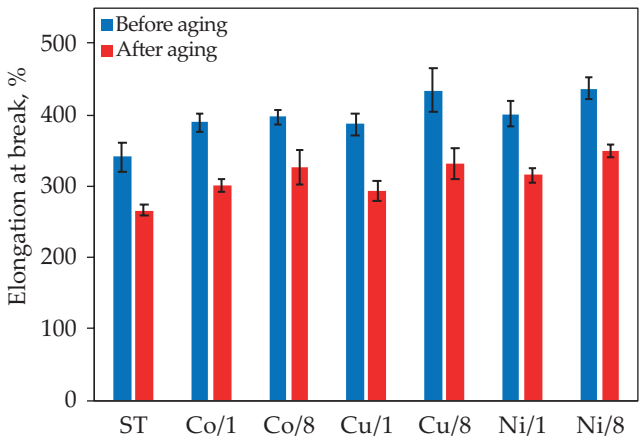

Fig. 9. Elongation at break before and after accelerated thermal aging in air

Table 4. Mechanical properties before and after accelerated thermal aging in air

Sample	Tensile strength, MPa		Elongation at break, %		Hardness, °ShA	
	Before	After	Before	After	Before	After
ST	17.8±1.3	17.6±0.5	341±20	266±8	60.4±0.3	64.2±1.2
Cu/1	18.7±0.8	18.0±0.8	387±13	293±8	60.0±0.6	64.7±1.2
Cu/8	19.5±0.6	17.8±0.9	434±9	332±24	58.6±0.5	63.5±0.2
Co/1	18.9±0.9	17.8±0.8	390±15	301±15	58.3±1.7	63.6±1.8
Co/8	18.8±1.3	17.6±1.2	397±30	327±22	60.5±0.1	63.3±0.7
Ni/1	18.4±0.9	17.5±0.4	401±18	315±9	59.2±0.4	62.0±1.9
Ni/8	19.2±0.6	18.6±0.8	437±15	349±9	58.9±0.5	63.0±0.7

The surface relief is distinctive, formed by a larger number of fragments of layers. Clearly demarcated segments on the surface of the layers are not largely observed. The individual layers are arranged more or less linearly. The thickness of the layers is smaller with small differences between the individual layers from which the particle is formed.

Processing parameters

Maximum and minimum torque data is shown in Table 3. It can be concluded that the addition of 1 phr modified kaolinite increased M_L, and the addition of 8 phr decreased.

In relation the M_L, refers to the stiffness of the rubber blend at the beginning of the curing or the stock modulus of filled rubber composite [39]. The increase in minimum torque (M_L) values of these blends compared with the standard mixture, can be associated with an incorporation of kaolinite particles between the rubber chains [38, 40].

The maximum torque (M_H) decreased significantly after the application of modified filler. This can be caused by the surface property and dispersion state of modified filler in rubber matrix [44]. In general, the maximum torque refers to the stiffness of the rubber composite at the end of curing process. The most comparable value could be seen in relation to the Co/1. According to the difference between the M_H and M_L, the degree of crosslinking can be characterized. As it can be seen in Table 3, the D*M* decreased significantly after the addition of modified kaolinite, mainly in relation to the Ni/8 and it could be attributed to the aggregation of particles on the surface of kaolinite. Thus, the tendency of M_H lowering can be assigned to the higher loading of modified kaolinite and could be attributed to the filler aggregation [45].

Curing characteristic

Scorch time, optimum curing time and curing time index are also presented in Table 3. The ignition time of blends containing modified kaolinite, except Cu/1 blend, was longer than t_{s2} of the reference blend (ST). From this point of view, it can be concluded, that the modification had a positive effect on scorch time. It can be seen that the modification of kaolinite shortens the optimal cure time, except for blends containing 1 phr KKA-Co and 8 phr KKA-Cu. The efficiency of the curing reactions by CRI can be seen. Furthermore, it can be seen that the CRI was smaller for Co/1 and Cu/8 blends. On the contrary, a significant decrease referring to the greatest CRI was seen for the Ni/8 blend. This effect can be caused by the increase of Lewis sites on the surface. In other words, large aggregation can prevent heat from flowing inwards [46].

Mechanical properties

Table 4 shows tensile properties and hardness of rubber blends with pure and modified kaolinite. It is observed that there is not any significant change of tensile strength observed before aging. However, some increase was observed. When evaluating the results of tensile strength, the loading of 8 phr (Ni/8 and Cu/8) showed greater increase, compared with ST. The higher tensile strength, mainly Cu/8, may be related to the larger surface area as well as to the increase in the homogeneity of the structure. On the other hand, a decrease in tensile strength after accelerated thermal aging is visible, but in terms of overall values, compared to the ST tensile strength after aging, it is still higher for all blends containing modified kaolinite. The same effect was observed for the elongation at break before and after accelerated thermal aging in air (Fig. 9). Herein, the KKA-Cu and KKA-Ni with loading of 8 phr showed greater increase and it can be associated with the increase of the rubber elasticity before the aging. Relating to the elasticity, the elongation at break describes the ability of material to be recovered after mechanical loading [36]. The same effect was observed for the elongation at break after the thermal aging for Cu/8 and Ni/8.

As presented in Table 4 the hardness of vulcanizates with modified kaolinite before and after the thermal aging were comparable with the ST. In relation to overall analysis of tensile properties, it was proved that the kaolinite modification stood for the optimum chemical treatment to achieve a partial substitution of carbon black. Based on above mentioned results, the addition of modified kaolinite improved the mechanical properties of rubber composites. Additionally, the explanation of the

improvement could be based on these statements: good interaction of the filler particles and rubber molecule chains, good dispersion and aggregation of new kaolinite filler in the rubber matrix, (according to the nature of used kaolinite, it is affected mainly by its surface characteristics), appropriate particle size and chemical interaction [47] between the Cu(II), Co(II), Ni(II), and kaolinite.

Also, the improvement could be caused by the fine dispersion of kaolinite particles. The presented findings could be also attributed to the constraint of the rubber chains motion due to the use of alternative filler [48, 49]. The increase of tensibility and elongation, mainly for higher loading of modified kaolinite, could be explained by the trapping of polymer chains between the kaolinite particles and forming of the bonded rubber, thus it could maintain higher stress [50].

CONCLUSIONS

The influence of kaolinite chemical modification with Co(II), Cu(II), and Ni(II) salts as a partial replacement for carbon black on the processing parameters and mechanical properties of the model rubber blend was investigated. FT-IR confirmed the formation of a complex of copper hydroxyacetate monohydrate, which may affect the chemical interactions between the rubber components and kaolinite at the curing temperature. The addition of modified kaolinite improved the processing parameters, tensile properties and hardness even after accelerated thermal aging in air. From this point of view, the modification of kaolinite with Cu(II) salt led to the desired change in properties, thanks to which KKA-Cu can be used as a partial replacement for carbon black.

ACKNOWLEDGMENT

The authors would like to thank the Slovak Grant Agency KEGA and VEGA for financial support (KEGA 001TNUAD-4/2022, VEGA 1/0265/24,). The work was supported by the project Advancement and support of R&D for Centre of Diagnostics and Quality Testing of Materials in the Domains of the RIS3 SK", ITMS2014+:313011W442.

Authors contribution

M.P. – conceptualization, supervision, validation, writing-review and editing; B.P. – methodology, investigation, conceptualization; D.O. – validation, supervision, methodology, writing-review and editing; J.V. – visualization, validation, conceptualization; A.F. – writing-original draft, investigation, methodology; S.D. – writing-original draft, investigation, methodology; A.D. – methodology, writing-original draft, investigation, Z.M. – investigation, methodology; T.W.K. – visualization, validation, conceptualization; D.C.K. – visualization, validation, conceptualization.

Funding

The work was funded by Slovak Grant Agency KEGA and VEGA (KEGA 001TNUAD-4/2022, VEGA 1/0265/24,). In addition, the work was supported by the project Advancement and support of R&D for Centre of Diagnostics and Quality Testing of Materials in the Domains of the RIS3 SK", ITMS2014+:313011W442.

Conflict of interest

The authors declare no conflict of interest.

REFERENCES

[1] Hemanth R., Sekar M., B. Suresha: *Indian Journal of Advances in Chemical Science* **2014**, *2*, 28.
[2] Zhang S., Liu Q., Cheng H. *et al.*: *Applied Clay Science* **2015**, *331*, 234. https://doi.org/10.1016/j.apsusc.2015.01.019
[3] Yang Y., Zhang H., Zhang K. *et al.*: *Applied Clay Science* **2020**, *185*, 105366. https://doi.org/10.1016/j.clay.2019.105366
[4] Zhang Y., Liu Q., Zhang Q. *et al.*: *Applied Clay Science* **2010**, *50*, 255. https://doi.org/10.1016/j.clay.2010.08.006
[5] Ramesh V., Rajarajan K.: *Mechanics, Materials Science and Engineering* **2017**, *9*. https://doi.org/10.2412/mmse.61.54.732
[6] Das A., Jurk R., Stöckelhuber K.W. *et al.*: *eXPRESS Polymer Letters* **2007**, *1(11)*, 717. https://doi.org/10.3144/expresspolymlett.2007.99
[7] Pavlidou S., Papaspyrides, C.D.: *Progress in Polymer Science* **2008**, *33(12)*, 1119. https://doi.org/10.1016/j.progpolymsci.2008.07.008
[8] Sheikh S.H., Yin X., Ansarifar A. *et al.*: *Journal of Reinforced Plastics and Composites* **2017**, *36(16)*, 1132. https://doi.org/10.1177/0731684417712070
[9] Raji V.V., Anitha A.M., Menon R.A.R.: *Polymer* **2016**, *89*, 135. https://doi.org/10.1016/j.polymer.2016.02.037
[10] Murray H.H.: *Clay Minerals* **1999**, *34*, 39. https://doi.org/10.1180/000985599546055
[11] de Macêdo Neto J.C., de Freitas B.M., de Miranda A.G. *et al.*: *Polymers* **2023**, *15(9)*, 2094. https://doi.org/10.3390/polym15092094
[12] Barton C.D., Karathanasis A.D.: "Clay Minerals" in "Encyclopedia of Soil Science", Volume 3, (Lal R.), Marcel Dekker, New York 2002, p. 187.
[13] Yaya A., Tiburu E.K., Vickers M.E. *et al.*: *Applied Clay Science* **2017**, *150*, 125. https://doi.org/10.1016/j.clay.2017.09.015

[14] Gasparini E., Tarantino S.C., Ghigna P. *et al.*: *Applied Clay Science* **2013**, *80–81*, 417. https://doi.org/10.1016/j.clay.2013.07.017
[15] Matusik J., Scholtzova E., Tunega D. *et al.*: *Clays and Clay Minerals* **2012**, *60(3)*, 227. https://doi.org/10.1346/CCMN.2012.0600301
[16] Li Y., Sun D., Pan X. *et al.*: *Clays and Clay Minerals* **2012**, *57(6)*, 779. https://doi.org/10.1346/CCMN.2009.0570610
[17] Garcia-Valles M., Puro A., Salvador M. *et al.*: *Minerals* **2020**, *10(2)*, 142. https://doi.org/10.3390/min10020142
[18] Bhattacharyya K.G., Gupta S.S.: *Advances in Colloid and Interface Science* **2008**, *140(2)*, 114. https://doi.org/10.1016/j.cis.2007.12.008
[19] Zuo X., Wang D., Zhang S. *et al.*: *Minerals* **2018**, *8(3)*, 112. https://doi.org/10.3390/min8030112
[20] Castrillo P.D., Olmos D., Sue H.J. *et al.*: *Composite Structures* **2015**, *133*, 70. https://doi.org/10.1016/j.compstruct.2015.07.040
[21] Makó E., Kovács A., Ható Z. *et al.*: *Journal of Colloid and Interface Science* ***2014***, *141*, 125. https://doi.org/10.1016/j.jcis.2014.06.006
[22] Makó E., Kovács A., Hotváth R. *et al.*: *Clay Minerals* **2014**, *49(3)*, 457. https://doi.org/10.1180/claymin.2014.049.3.08
[23] Ogbebor O.J., Okieimen F.E., Okwu D.E.: *Chemical Industries and Chemical Engineering Quarterly* **2015**, *21(4)*, 477. https://doi.org/10.2298/CICEQ140221003O
[24] Mukhopadhyay R. Sarkar B., Palansooriya K.N. *et al.*: *Advances in Colloid and Interface Science* **2021**, *297*, 102537. https://doi.org/10.1016/j.cis.2021.102537
[25] Saikia B.J., Parthasarathy G.: *Journal of Modern Physics* **2010**, *1(4)*, 206. https://doi.org/10.4236/jmp.2010.14031
[26] Prasad M.S., Reid K.J., Murray H.H.: *Applied Clay Science* **1991**, *6(2)*, 87. https://doi.org/10.1016/0169-1317(91)90001-P
[27] Sun D., Li Y., Zhang B. *et al.*: *Composite Science and Technology* **2010**, *70(6)*, 981. https://doi.org/10.1016/j.compscitech.2010.02.016
[28] Yener N., Biçer C., Önal M. *et al.*: *Applied Surface Science* **2012**, *258(7)*, 2534. https://doi.org/10.1016/j.apsusc.2011.10.088
[29] Rutkai G., Makó É., Kristóf T.: *Journal of Colloid and Interface Science* **2009**, *334(1)*, 65. https://doi.org/10.1016/j.jcis.2009.03.022
[30] Cheng H., Liu, Q., Yang J. *et al.*: *Applied Clay Science* **2010**, *50(4)*, 476. https://doi.org/10.1016/j.clay.2010.09.011
[31] Cheng H., Liu Q., Yang J. *et al.*: *Thermochimica Acta* **2012**, *545*, 1. https://doi.org/10.1016/j.tca.2012.04.005
[32] Komori Y., Sugahara Y., Kuroda K.: *Applied Clay Science* **1999**, *15(1-2)*, 241. https://doi.org/10.1016/S0169-1317(99)00014-9
[33] Mbey J.A., Thomas F., Ngally Sabouang C.J. *et al.*: *Applied Clay* Science **2013**, *83–84*, 327. https://doi.org/10.1016/j.clay.2013.08.010
[34] Valášková M., Rieder M., Matějka V. *et al.*: *Applied Clay Science* **2007**, *35(1–2)*, 108. https://doi.org/10.1016/j.clay.2006.07.001
[35] Feriancová A., Pajtášová M., Pecušová B. *et al.*: *Applied Clay Science* **2019**, *183*, 105313. https://doi.org/10.1016/j.clay.2019.105313
[36] Qin L., Zhang Y., Zhang Y. *et al.*: *Applied Clay Science* **2021**, *213*, 106237. https://doi.org/10.1016/j.clay.2021.106237
[37] Kloprogge J: "Spectroscopic Methods in the Study of Kaolin Minerals and Their Modifications", Springer, Cham 2019, p. 428.
[38] Zhang A., Zhang Y., Zhang Y.: *Polymer Testing* **2020**, *89*, 106600. https://doi.org/10.1016/j.polymertesting.2020.106600
[39] Feriancová A., Dubec A., Pagáčová J. *et al.*: *Applied Clay Science* ***2021***, *213*, 106259. https://doi.org/10.1016/j.clay.2021.106259
[40] Cheng H., Liu Q., Cui X. *et al.*: *Journal of Colloid and Interface Science* **2012**, *376(1)*, 47. https://doi.org/10.1016/j.jcis.2012.02.065
[41] Pajtášová M., Ondrušová D., Jóna E. *et al.*: *Journal of Thermal Analysis and Calorimetry* **2010**, *100*, 769. https://doi.org/10.1007/s10973-010-0769-x
[42] Tironi A., Trezza, M.A., Irassar E.F. *et al.*: *Procedia Materials Science* **2012**, *1*, 343. https://doi.org/10.1016/j.mspro.2012.06.046
[43] Nelson P.N., Taylor R.A.: *Applied Petrochemical Research* **2014**, *4*, 253. https://doi.org/10.1007/s13203-014-0044-3
[44] Zhang Y., Liu Q., Zhang S. *et al.*: *Applied Clay Science* **2016**, *124–125*, 167. https://doi.org/10.1016/j.clay.2016.02.002
[45] Wu S., Zhang Y., Zhang Y. *et al.*: *Applied Clay Science* **2022**, *216*, 106342. https://doi.org/10.1016/j.clay.2021.106342
[46] Flessner U. Jones D.J., Rozière J. *et al.*: *Journal of Molecular Catalysis A: Chemical* **2001**, *168(1–2)*, 247. https://doi.org/10.1016/S1381-1169(00)00540-9
[47] Wang Y., Zhang H., Wu Y. *et al.*: *European Polymer Journal* **2005**, *41(11)*, 2776. https://doi.org/10.1016/j.eurpolymj.2005.05.019
[48] Pajtášová M., Mičicová Z., Ondrušová D. *et al.*: *Procedia Engineering* **2017**, *177*, 470. https://doi.org/10.1016/j.proeng.2017.02.247
[49] Anastasiadis S.H., Chrissopoulou K., Frick B.: *Material Science and Engineering: B* **2008**, *152(1–3)*, 33. https://doi.org/10.1016/j.mseb.2008.06.008
[50] Liu Q., Zhang Y., Xu H.: *Applied Clay Science* **2008**, *42(1–2)*, 232. https://doi.org/10.1016/j.clay.2007.12.005

Received 20 II 2024.
Accepted 15 III 2024.